Journal of Experimental Botany Advance Access published December 10, 2016

Journal of Experimental Botany
doi:10.1093/jxb/erw429

RESEARCH PAPER

Overexpression of *AtERF019* delays plant growth and senescence and improves drought tolerance in Arabidopsis

Telma E. Scarpeci, Vanesa S. Frea, María I. Zanor and Estela M. Valle

Instituto de Biología Molecular y Celular de Rosario (IBR-CONICET-UNR), Ocampo y Esmeralda, Predio CCT, Rosario 2000, Argentina

Correspondence: valle@ibr-conicet.gov.ar

Received 7 September 2016; Editorial decision 25 October 2016; Accepted 4 November 2016

Editor: Peter Bozhkov, Swedish University of Agricultural Sciences, Sweden

Abstract

The transcription factor superfamily, APETALA2/ethylene response factor, is involved in plant growth and development, as well as in environmental stress responses. Here, an uncharacterized gene of this family, *AtERF019*, was studied in *Arabidopsis thaliana* under abiotic stress situations. Arabidopsis plants overexpressing *AtERF019* showed a delay in flowering time of 7 days and a delay in senescence of 2 weeks when comparison with wild type plants. These plants also showed increased tolerance to water deficiency that could be explained by a lower transpiration rate, owing to their smaller stomata aperture and lower cuticle and cell wall permeability. Furthermore, using a bottom-up proteomic approach, proteins produced in response to stress, namely branched-chain-amino-acid aminotransferase 3 (BCAT3) and the zinc finger transcription factor oxidative stress 2, were only identified in plants overexpressing *AtERF019*. Additionally, a *BCAT3* mutant was more sensitive to water-deficit stress than wild type plants. Predicted gene targets of AtERF019 were *oxidative stress 2* and genes related to cell wall metabolism. These data suggest that AtERF019 could play a primary role in plant growth and development that causes an increased tolerance to water deprivation, so strengthening their chances of reproductive success.

Key words: Arabidopsis, AtERF019, cell wall, drought stress, ERF transcription factor, oxidative stress, proteomics, senescence.

Introduction

Water deficit is considered the most serious environmental factor limiting crop productivity worldwide (Boyer, 1982). Water-deficit stress triggers responses ranging from changes in gene expression patterns to changes in metabolism and plant growth. These responses can be adaptive, such as inhibition of lateral root growth (Xiong *et al.*, 2006), but they can also promote survival, such as regulating cell proliferation and expansion (Claeys and Inzé, 2013). Under water-deficit stress plants arrest shoot growth, a process that involves cell wall synthesis and remodeling (Tenhaken, 2015). Other effects of water limitation in plants include decreased transpiration and photosynthesis (Boyer and Bowen, 1970) and foliar senescence (Buchanan-Wollaston *et al.*, 2003; Buchanan-Wollaston *et al.*, 2005). The induction of leaf senescence by water deficiency contributes to plant survival since nutrients from senescent leaves are transported to young leaves and reproductive organs. Furthermore, non-productive leaves are eliminated by abscission, causing a reduction of water loss by transpiration. Plants therefore use senescence as a strategy to withstand stress conditions (Munné-Bosch and Alegre, 2004;

Abbreviations: ALDH, betaine aldehyde dehydrogenase; AP2, apetala2; AtBGAL10, β-galactosidase Galactosidase 10; AtNUDX2, nudix hydrolase 2; BCAT3, branched-chain-amino-acid aminotransferase 3; BCAAs, branch-chain amino acids; CaMV, cauliflower mosaic virus; EAR, ERF-associated amphiphilic repression; ERF, ethylene response factor; FDR, false discovery rate; GS, glutamine synthetase; LSU, large subunit; MTHFR2, methylenetetrahydrofolate reductase 2; MS, Murashige and Skoog; OXS2, oxidative stress 2; qPCR, quantitative real-time PCR; RTNLB2, reticulon-like protein B2; SOD, superoxide dismutase

Lers, 2007). Suppression of drought-induced leaf senescence was previously observed in transgenic plants expressing a gene encoding an isopentenyltransferase (Rivero *et al.*, 2007). This demonstrated the existence of a relationship between water-deficit stress and senescence.

Plants respond to unfavorable environments by expressing stress-related genes such as transcription factors to survive, grow and reproduce (Osakabe *et al.*, 2014). Altering the expression of transcription factors in plants through genetic engineering can affect several signaling pathways and improve abiotic stress tolerance (Wang *et al.*, 2016). In a previous study, it was found that members of common transcription factor families were highly induced when *Arabidopsis thaliana* plants were treated with methyl viologen, a superoxide anion propagator generated during photosynthesis (Scarpeci *et al.*, 2008). Among these transcription factors was a member of the APETALA2 (AP2)/ethylene response factor (ERF) family, *AtERF019*. *AtERF019* showed the highest induction after oxidative stress (Scarpeci *et al.*, 2008). *AtERF019* transcripts were also induced by hydrogen peroxide as shown in genome-wide transcriptomic analyses of a catalase loss-of-function mutant exposed to high light stress (Vanderauwera *et al.*, 2011; Inze *et al.*, 2012). These findings indicate that *AtERF019* plays a role in oxidative stress, although its function is so far uncharacterized. AP2/ERF transcription factors are involved in growth, development and hormone responses, with most of them also helping to regulate responses to biotic and abiotic stress (Abogadallah *et al.*, 2011; Mizoi *et al.*, 2012; Licausi *et al.*, 2013; Cao *et al.*, 2015). AP2/ERF transcription factors function in drought and high salinity (Fujimoto *et al.*, 2000), and their overexpression in transgenic plants can confer tolerance to salt and pathogens (Park *et al.*, 2001). These transcription factors contain AP2/ERF-type DNA binding domains, and family members are encoded by 147 loci in Arabidopsis (Sakuma *et al.*, 2002; Nakano *et al.*, 2006). Based on conserved motifs outside the DNA-binding domain, the ERF transcritption factor family can be further divided into several distinct groups (Sakuma *et al.*, 2002; Nakano *et al.*, 2006; Licausi *et al.*, 2013). Group II/A-5 contains stress-inducible genes in Arabidopsis (Mizoi *et al.*, 2012), and its members are further classified into three subgroups, IIa, IIb, and IIc (Nakano *et al.*, 2006). In addition to the AP2/ERF domain, subgroup IIa members contain a motif called CMII-2 at their C-terminus, which is similar to the ERF-associated amphiphilic repression (EAR) motif. The CMII-2 motif enables transcriptional repression of downstream target genes (Nakano *et al.*, 2006, Li *et al.*, 2011). Members of subgroup IIa, such as RAP2.1, RAP2.9 and RAP2.10, were reported to be transcriptional repressors that modulate stress responses (Tsutsui *et al.*, 2009; Dong and Liu, 2010; Amalraj *et al.*, 2016). Characteristic of subgroups IIb and IIc is the absence of the CMII-2 motif (Nakano *et al.*, 2006). AtERF019 belongs to subgroup IIc together with *At1g71520*, the closest homolog in Arabidopsis (Nakano *et al.*, 2006). The EAR motif is also present in members of group VIIIa, such as in the repressor ERF11 (Ohta *et al.*, 2001; Dubois *et al.*, 2015; Zhou *et al.*, 2016). Ectopic overexpression of *ERF* genes led to growth impairment in several cases, but in others it led to improved performance in terms of survival and yield when subjected to stress treatments (Licausi *et al.*, 2013). In particular, overexpression of *ERF6*, a member of subgroup IXb of the ERF family, caused dwarfism. However overexpression of *ERF11* antagonized this effect (Dubois *et al.*, 2015), providing a mechanism to maintain the balance between plant growth and stress tolerance upon exposure to stress.

The aim of this study was to investigate the function of AtERF019 under abiotic stress in Arabidopsis. Plants overexpressing *AtERF019,* refered to hereafter as ERF019 lines, showed slower plant growth and development, delayed natural senescence, and enhanced drought tolerance when compared with wild type plants, refered to hereafter as Col-0. To further investigate the different drought response of ERF019 plant lines and Col-0 a bottom-up proteomic analysis was performed. Differences in protein expression were particularly evident for proteins known to be produced in response to stress and proteins related to cell wall metabolism. Among proteins associated with stress were the branched-chain-amino-acid aminotransferase 3 (BCAT3) and the zinc finger transcription factor oxidative stress 2 (OSX2). Regarding cell wall metabolism, the following enzymes were identified as more abundant in ERF019 plant lines when comparison with Col-0 under control or water-deficit stress conditions: methylenetetrahydrofolate reductase 2 (MTHFR2); callose synthase 12 (CalS12); endoglucanase 25 (also known as KORRIGAN) and β-Galactosidase 10 (AtBGAL10). Additionally, the genes encoding these proteins, with the exception of *BCAT3*, are all predicted targets of AtERF19.

Materials and Methods

Plant material

Arabidopsis thaliana (L.) Heynh. Col-0 seeds were sown in soil in 10 cm pots or 0.5x Murashige and Skoog (MS) medium (Sigma, St Louis, USA) containing 0.8% (w/v) agar. They were grown in a controlled environment chamber under a 16 h light/8 h dark photoperiod using fluorescent light at 120 µmol m^{-2} s^{-1} at 23 ± 2 °C and a relative humidity of 65–70%.

AtERF019 *cloning and plant transformation*

PCR was used to amplify the *AtERF019* coding region using Arabidopsis Col-0 flower cDNA as template and two specific primers (see Supplementary Table S1 at *JXB* online). To generate the ERF019 construct, sequence fidelity of *AtERF019* cDNA was confirmed by DNA sequencing (at the University of Maine DNA sequencing facility, USA, Orono, ME) and it was inserted downstream of the cauliflower mosaic virus (CaMV) 35S promoter in a modified pGreen 0229 binary expression vector using *Pac*I and *Pme*I sites (Skirycz *et al.*, 2006). *Agrobacterium tumefaciens* strain GV3101 (pMP90) was transformed with this construct and used to obtain transgenic Arabidopsis plants using the floral dip procedure (Clough and Bent, 1998). Selection was performed on plants growing in soil by spraying 5-day-old seedlings with a 300 µM Basta (glufosinate ammonium, Sigma) working solution. The treatment was repeated twice at three day intervals. Segregation analysis was performed using the Chi-square statistical test to select those lines with one T-DNA copy. Homozygous T3 transgenic lines were used for these studies.

Quantitative real-time PCR (qPCR)

Total RNA was extracted from leaves of Col-0 and ERF019 plants using TRIzol (Invitrogen Life Technologies, Argentina) following the manufacturer's procedure. Quality and quantity of RNA, as well as RNA reverse transcription and qPCR, were performed as previously described (Scarpeci *et al.*, 2013). The primers used are listed in Supplementary Table S1.

Chlorophyll fluorescence

Three-week-old plants of Arabidopsis were dark-adapted for 30 min before measurements. Chlorophyll fluorescence was measured at 23 °C employing a Qubit Systems Inc. pulse-modulated fluorometer (Kingston, Canada). The maximum quantum efficiency, Fv/Fm, was calculated as described (Baker and Rosenqvist, 2004).

Stomatal aperture

For measurements, the third and fourth leaf from 21-day-old plants of ERF019 and Col-0 were used, grown under optimal conditions of temperature and humidity. Silicon rubber impressions were taken from leaves by mixing equal parts of silicone impression material and hardener (Zhermack, Marl, Germany) and immediately applied to the abaxial surface of the leaves using minimal pressure (Weyers and Johansen, 1985). After hardening, a positive impression was made covering the silicone imprints with a thin layer of nail varnish and leaving it to dry for at least 1 h and then placing the positive impression on a glass slide. Photographs of stomata were taken using a light microscope (Olympus BH-2, Tokyo, Japan). The width and length of 30–40 stomatal apertures in ten leaves for each line were measured with the image processing software Image J (http://imagej.nih.gov/ij/). The ratios between these measurements were calculated, averaged, and statistically analyzed using a one-way ANOVA test.

Water-deficit stress survival analysis

Two to three seeds from plants of ERF019 lines and Col-0 were sown in 180 cm^3 pots containing the same weight of air-dried soil [60 g GrowMix Multipro soil: 85–90% organic matter, 30–35% available water capacity, pH 5.2–5.8 (Terrafertil, Moreno, Argentina)]. Plants were grown in soil under optimal conditions (as stated in the Materials and Methods, under Plant material) for 21 days. At this age, no water was added until stress became evident, such as the appearance of wilted chlorotic leaves, usually after approximately a further 17 days. During the water-deficit stress treatment, the water content of leaves and soil dropped gradually, starting with plants with a water content of 0.93 g H_2O g FW^{-1} when soil was saturated with water (100%) and ending with 0.81 g H_2O g FW^{-1} when soil water content was 25% of the initial value. Ten plants per genotype were tested, and the experiment was performed twice. Photographs were taken two days after re-watering and the survival rates of ERF019 lines and Col-0 were calculated. A z-test for proportions (Sprinthall, 2002) was used to test the statistical difference in survival rate between Col-0 and ERF019 lines.

Dark-induced leaf senescence

Dark-induced senescence triggered in Arabidopsis was performed with plants grown in soil or MS, as described above, following published procedures (Ülker et al., 2007; Yang *et al.*, 2011) with modifications. For plants grown in soil (Ülker *et al.*, 2007), rosettes of 21-day-old plants were excised and placed into microtiter plates on sterile filter paper moistened with water. The plates were kept in darkness for three days at 22 °C. For plants grown on MS-agar (Yang *et al.*, 2011) 10-day-old seedlings were transferred to complete darkness for six days in the growing chamber.

Determination of pigment content

Pigments were extracted from leaves with 96% (v/v) ethanol. The supernatant was used to measure chlorophyll *a*, chlorophyll *b* and carotenoids content (Lichtenthaler *et al.*, 1986).

For chlorophyll leaching assays, roots and inflorescence stems of four-week-old plants were cut off and the remaining rosette was weighed, put in tubes containing 20 mL of 80% ethanol and 10 mM MES pH 5.8 at room temperature and gently agitated in the dark. Fifty microliters were removed from each sample every 20 min. Absorbance measured at 665 and 645 nm was used to calculate micrograms of total chlorophyll per gram of FW of tissue.

Determination of proline content

Proline was determined according to (Bates *et al.*, 1973) with modifications. Twenty milligrams of Arabidopsis leaves were extracted twice with 80% (v/v) ethanol with 10 mM MES pH 5.9 and once with 50% (v/v) ethanol with 10 mM MES pH 5.9. Each extraction step was performed for 30 min at 80 °C and the supernatants were combined. For Pro determination, 100 µL of the ethanol extract or Pro standard were mixed with 100 µL ninhydrin reagent [1% (w/v) ninhydrin in 60% (v/v) acetic acid] and heated at 95 °C for 20 min. Absorbance measured at 520 nm was used to calculate µmol of Pro per gram of FW tissue.

Protein blot analysis

For extraction of soluble proteins, leaves were homogenized with 50 mM potassium phosphate pH 7.5, 1 mM phenylmethylsulfonyl fluoride, 15% (v/v) glycerol and 2% (w/v) polyvinylpolypyrrolidone. Proteins in solution were quantified spectrophotometrically using Coomassie brilliant blue G250 dye (Sigma) and BSA as the standard for the calibration curves (Sedmak and Grossberg, 1977). Leaf proteins were resolved on 12% SDS-PAGE, transferred to nitrocellulose membranes and immunoreacted with polyclonal antibodies raised against glutamine synthetase (GS) (Scarpeci *et al.*, 2007) or stained using Coomassie brilliant blue R250 (Sigma). Densitometric analyses were done using Image J software (http://imagej.nih.gov/ij/).

Native PAGE and activity staining

Extraction of soluble proteins for superoxide dismutase (SOD) activity was done according to a published procedure (Gupta *et al.*, 1993). Twenty-five micrograms of soluble protein from leaf extracts were subjected to native PAGE. SOD activity was assayed in the gel according to (Beauchamp and Fridovich, 1971).

Controlled water-deficit stress treatment

Water-deficit stress was applied according to (Hummel *et al.*, 2010) with modifications. Seeds of Col-0 and ERF019 lines were sown in 200 mL cylindrical plastic pots filled with soil. Each pot was weighed daily and its soil water content kept constant at a control level of 0.35 to 0.40 g water g^{-1} dry soil at 100% humidity. Twenty-one days after sowing, half of the plants were kept well-watered until they were harvested (control plants), while for the other half irrigation was stopped until the soil water content reached a target of 65 to 70% humidity, corresponding to a moderate water deficit. Once the target soil water content was reached, it was kept constant with daily watering. After fifteen days, pools of 4–5 plants of control or treated plants were harvested at the end of the photoperiod, frozen in liquid nitrogen, and later used for protein extraction and determination of pigment and proline contents.

Protein extraction under denaturing conditions

Approximately 0.5 g of leaves were ground in liquid nitrogen using a mortar and pestle, transferred to a tube containing 1.25 mL of extraction buffer [100 mM Tris-HCl, pH 8.8, 2% (w/v) SDS, 0.4% (v/v) 2-mercaptoethanol, 10 mM EDTA, 1 mM phenylmethylsulfonyl fluoride, and 0.9 M sucrose] and 1.25 mL of phenol saturated with ice-cold Tris-HCl at pH 8.8 (Invitrogen, Buenos Aires, Argentina), and then agitated at 4 °C for 30 min. Tubes were centrifuged at

20 000 × g for 10 min at 4 °C. The phenolic phase was transferred to a new tube, leaving the interface intact. The aqueous phases were back extracted with 1 mL extraction buffer and 1 mL phenol, vortexed and the tubes then centrifuged at 20 000 × g for 10 min at 4 °C. The phenolic phase was combined with the previous phenolic phase. Proteins were precipitated with 5 volumes of 0.1 M cold ammonium acetate in methanol at -20 °C overnight. Samples were collected by centrifugation at 20 000 × g at 4 °C for 20 min. Next, the pellet was washed twice with 1.5 mL of 0.1 M cold ammonium acetate in methanol and once with 70% (v/v) cold methanol. Finally, the pellet was dried and solubilized in a buffer containing 4% SDS, 100 mM Tris-HCl, pH 7.5 and 10 mM DTT.

Gel-based proteomic analysis

The procedure developed by (Bumpus *et al.*, 2009) was followed with modifications. An aliquot of the total protein extract (15 µg) was loaded onto an SDS-PAGE gel (Tris-HCl gradient gel, 4 to 20%, Biorad, California, USA). The gel was silver stained (Thermo Fisher, Massachusetts, USA), each gel lane cut with a razor blade into 12 bands and then chopped into small pieces. These gel samples were destained (Thermo), reduced with 10 mM DTT (Sigma), alkylated with 55 mM iodoacetamide (Sigma) and digested with trypsin (Promega, Madison, USA). Peptides were extracted, dried down and resuspended in 30 µL 5% acetonitrile and 0.2% formic acid. Peptide products were analyzed by reverse phase nanoLC-MS/MS Velos Orbitrap (Thermo Fisher). Protein identification was achieved by reference to the TAIR 8 database using Mascot and Scaffold softwares. Proteins were identified using Scaffold software. Data was estimated to have a 0.1% false discovery rate (FDR) at the protein level and 0.3% FDR at the peptide level.

Software and data analyses

The mass spectrometry RAW files were processed with Crawler software (Neil Kelleher Research Group, Northwestern University, USA) to assign masses. Using this program, both the intact masses and the corresponding fragment masses were determined and these data searched against an Arabidopsis proteome database. Extensive statistical workups were also performed using several FDR estimation approaches, with both concatenated and non-concatenated decoy databases.

Tandem mass spectrometry samples were analyzed using Mascot (Matrix Science, London, UK). Mascot was set up to search the SwissProt_2012_06 database, with 11247 entries when selected for *Arabidopsis thaliana*. Mascot was searched with a fragment ion mass tolerance of 0.80 Da and a parent ion tolerance of 10.0 ppm. Iodoacetamide derivative of cysteine was specified in Mascot as a fixed modification. Oxidation of methionine and phosphorylation of serine, threonine and tyrosine were specified in Mascot as variable modifications.

Scaffold (version Scaffold_3.6.1, Proteome Software Inc., Portland, USA) was used to validate tandem mass spectrometry-based peptide and protein identifications. Peptide identifications were accepted if they could be established at greater than 95.0% probability as specified by the Peptide Prophet algorithm (Keller *et al.*, 2002). Proteins were considered positively identified if a 99.0% probability of correct identification could be established in at least two unique peptides. Protein probabilities were assigned by the Protein Prophet algorithm (Nesvizhskii *et al.*, 2003). Proteins that contained similar peptides and could not be differentiated based on tandem mass spectrometry analysis alone were grouped to satisfy the principles of parsimony.

Statistical analysis

Experimental data were subjected to z-test or ANOVA analysis with lines as factors, followed by a Holm-Sidak or Dunnett significant difference *post hoc* test using Sigma Plot software (version 11.0). A P value less than 0.05 was considered statistically significant. Model assumptions were tested by analysis of residuals. All experiments were done at least three times.

Results

Phenotypic characterization of transgenic Arabidopsis plants overexpressing AtERF019

To assess the function of the transcription factor AtERF019, transgenic Arabidopsis plants that constitutively express *AtERF019* (*At1g22810*) under the control of the CaMV 35S promoter were generated. More than 20 independent ERF019 lines were obtained; four T3 homozygous ERF019 lines with a higher level of *AtERF019* transcripts than Col-0 were selected for further studies (Fig. 1A and B). It is worth mentioning that the level of endogenous *AtERF019* expression under optimal growth conditions in Col-0 plants is very low, as previously shown by Northern blot analysis (Scarpeci *et al.*, 2008). Consequently the contribution of endogenous *AtERF019* transcripts to the qPCR values is negligible compared to the level of *AtERF019* transgene expression. Under optimal growth conditions, these ERF019 lines showed downward leaf curling and smaller rosette size compared with Col-0 plants (Fig. 1A, Supplementary Fig. S1). This observation was corroborated by measuring the FW of 21-day-old plants grown under optimal conditions (Fig. 1C). ERF019-6 and ERF019-7 plant lines had significantly lower FW than Col-0 plants at 35 ± 3 mg and 57 ± 3 mg, respectively). The alterations in leaf development observed in ERF019 lines led us to analyze the complexity of cotyledons venation according to the classification carried out by (Semiarti *et al.*, 2001). Among Col-0 cotyledons, 80% were classified as type I and 20% as type II (see Supplementary Fig. S2A). By contrast, 59% of ERF019-6 cotyledons and 48% of ERF019-7 cotyledons were of type II. None of the lines analyzed presented type III cotyledons (Supplementary Fig. S2A). Another characteristic of ERF019 lines was a significant reduction in the angle formed between the silique and the inflorescence stem in relation to Col-0 plants (Supplementary Fig. S2B). Concerning pigment levels, there were no statistically significant differences in chlorophyll and carotenoids levels among the plants analyzed except for the ERF019-8 line that presented a significantly higher level of chlorophyll *a* in 15-day-old plants and chlorophyll *a* and chlorophyll *b* in 30-day-old plants (see Supplementary Fig. S3).

Effects of AtERF019 *overexpression on natural senescence and dark- induced leaf senescence*

AtERF019 overexpression extends the duration of vegetative growth by 7 days in comparison to Col-0 plants and therefore increases the number of leaves formed before flower development (Supplementary Fig. S1). Additionally, the overexpression of *AtERF019* delayed the onset of leaf senescence and extended the lifespan of the plants by approximately 2 weeks compared with that of Col-0 plants (Fig. 2A). This observation was evaluated by measuring different senescence-associated

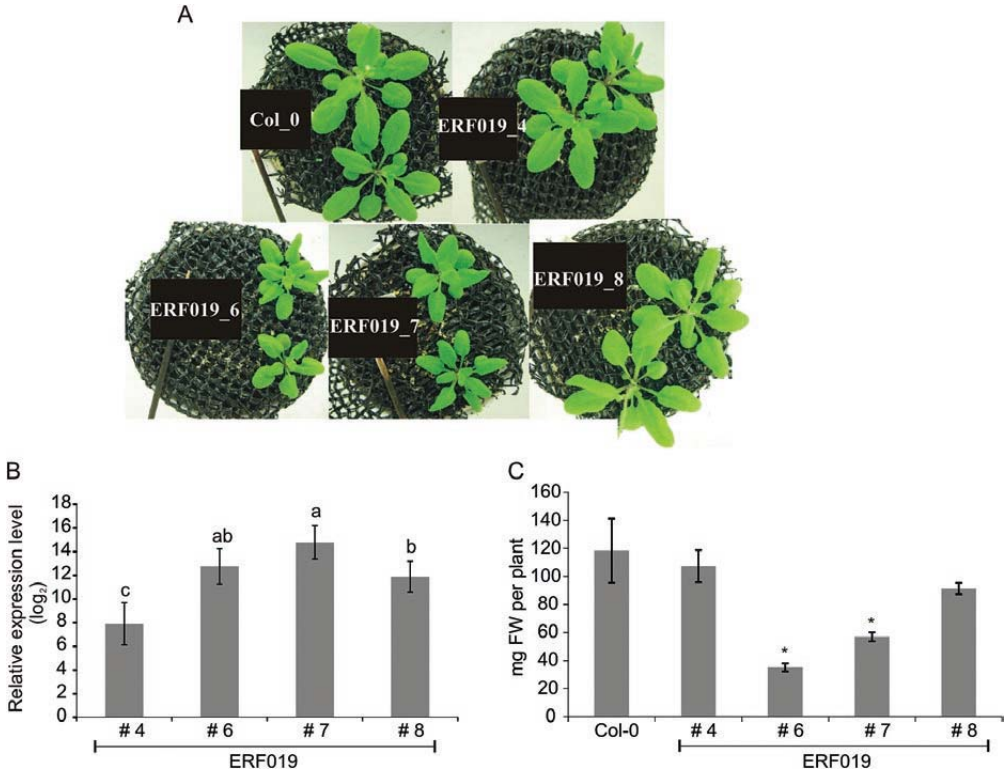

Fig. 1. Transgenic plants constitutively overexpressing *AtERF019*. (A) Representative photographs of 21-day-old plants of ERF019-4, -6, -7 and -8 lines and Col-0. (B) Relative abundance (log_2) of *AtERF019* transcripts in the leaves of ERF019 lines in comparison to Col-0 plants. The error bars indicate the SE (n=3). Different lower-case letters (a, b or c) show significant differences among lines. (C) FW of the aerial part of 21-day-old plants of ERF019 and Col-0 grown in soil in a growth chamber with 16 h daylight and under optimal conditions of light, temperature and humidity. The results are expressed in mg of FW per plant. The error bar indicates the SE (n=3). The asterisks over the error bars indicate a significant difference between plants of ERF019 lines and Col-0 (P<0.003). (This figure is available in colour at *JXB* online.)

physiological markers, such as chlorophyll and soluble protein content as well as Rubisco large subunit (LSU) and glutamine synthetase levels. Photosynthetic pigments were measured on a DW basis in 63-day-old plants. All ERF019 lines, except ERF019-4, showed statistically significant higher levels of chlorophyll content when compared with Col-0 plants (Fig. 2B). There were no statistically significant differences in carotenoids levels among the plants analyzed (data not shown). Besides chlorophyll depletion, protein depletion is an important senescence marker (Dangl *et al.*, 2000). Total protein content was determined in 63-day-old leaves of ERF019 and Col-0. ERF019-8 and ERF019-7 lines showed the highest protein content (25 ± 3 and 22 ± 2 mg protein g^{-1} DW, respectively) compared to Col-0 (9 ± 1 mg protein g^{-1} DW) (Fig. 2C). Rubisco is the most abundant protein in leaves and its degradation starts at the onset of senescence to generate source of nitrogen. The level of Rubisco in senescent plants was analyzed by SDS-PAGE of leaf extracts on a DW base (Fig. 2D). Rubisco LSU levels were higher in ERF019 lines in comparison to Col-0 plants. ERF019-8 showed the highest band intensity, followed by ERF019-7, ERF019-6, and ERF019-4 plant lines.

In parallel, these leaf extracts were used in an immunoblot assay to detect levels of the glutamine synthetase isoforms, GS1 (cytosolic isoform) and GS2 (chloroplastic isoform) (Fig. 2E). Densitometry analysis revealed that leaves of ERF019-6, -7 and -8 lines had twice the levels of GS2 when compared with ERF019-4 and Col-0 plants. Relative to GS1, GS2 band intensity was two-fold higher in ERF019-6, -7 and -8 lines and two-fold lower in ERF019-4. In Col-0 plants, GS1 and GS2 levels were similar to each other but relative to ERF019 lines were lower (Fig. 2E).

To corroborate the delay in natural senescence observed in ERF019 lines, dark-induced senescence assays were performed with 21-day-old plants of Col-0 and transgenic lines grown in soil. After three days in darkness, Col-0 plants showed a severe yellowing while ERF019 lines had a slight discoloration. Additionally, total chlorophyll content (Fig. 3A) and Rubisco LSU (Fig. 3B) were higher in transgenic plants than in Col-0 plants, with ERF019-8 showing the highest values. There was no change in carotenoids levels in the different plants analyzed (data not shown). To examine whether this phenotype depends on the developmental stage of the plant, seedlings grown on 0.5x MS-agar for ten days were placed in darkness in the plant growth chamber for six days. No significant differences in the chlorophyll content of the aerial plant tissues were detected between the transgenic and Col-0 plants (see Supplementary Fig. S4).

ERF019 plants showed increased tolerance to water-deficit stress

The expression level of *AtERF019* under different conditions was explored using the GENEVESTIGATOR database

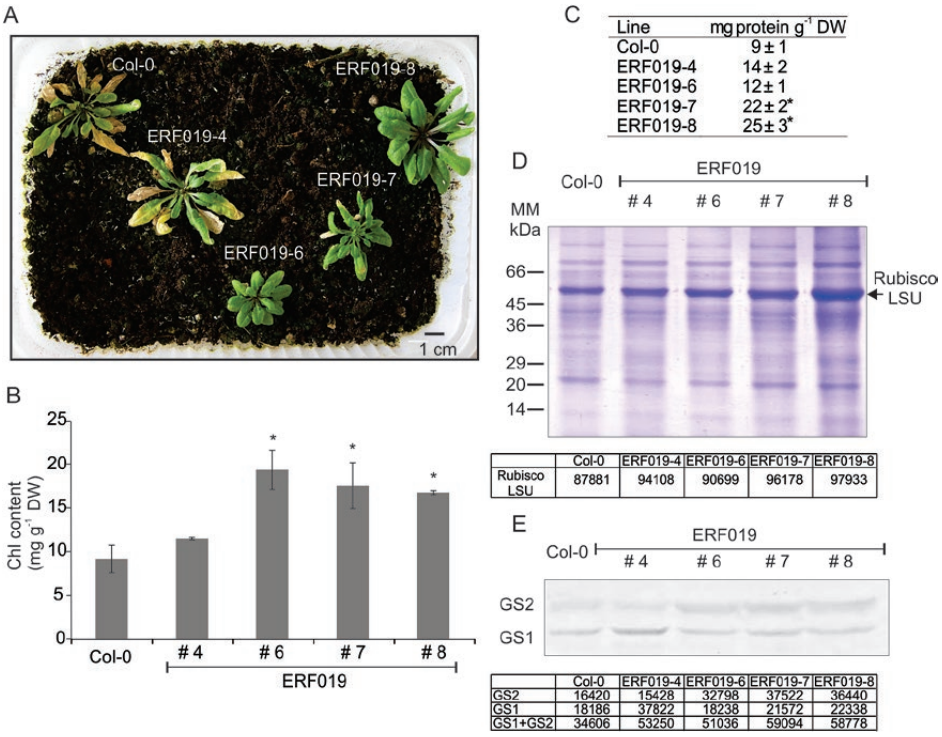

Fig. 2. Characterization of 63-day-old senescing plants of ERF019 lines. (A) Representative photographs of plants of ERF019 and Col-0 grown in soil under optimal conditions of light, temperature and humidity. The inflorescences were removed to observe the phenotype. (B) Total chlorophyll content corresponding to Col-0 and ERF019 lines. The values are given as mg of total chlorophyll per 1 g of leaf DW. The error bars indicate the sample SE (n=3). The asterisks over the error bars indicate a significant difference between plants of ERF019 lines and Col-0 (P<0.007). (C) Total protein content of Col-0 and ERF019 lines. The asterisks indicate a significant difference between plants of ERF019 lines and Col-0 (P<0.005). (D) Coomassie blue-stained SDS-PAGE gel showing the difference in protein content among the different plants of Col-0 and ERF019 lines. Each line contains protein extracts corresponding to 0.5 mg DW from Col-0 and ERF019-4, -6, -7 and -8 senescent leaves. The position of molecular mass markers (MM), in kDa, is shown on the left. An arrow indicates the position of Rubisco LSU. The table below shows Rubisco LSU relative abundance quantified by digitalization normalized to mg of DW and expressed as a ratio of arbitrary units for pixel intensities. (E) Immunoblot showing the presence of GS1 (cytosolic isoform) and GS2 (chloroplastic isoform) in senescent leaves of ERF019 lines and Col-0. Each line contains protein extracts corresponding to 5 mg DW from Col-0 and ERF019-4, -6, -7 and -8 senescent leaves. The table below shows GS relative abundance quantified by digitalization as described above.

(Zimmermann *et al.*, 2004). *AtERF019* is highly induced in Arabidopsis by biotic and abiotic treatments such as the introduction of a bacterial elicitor, water-deficit or unfavourable salt conditions (see Supplementary Fig. S5). The abilty of ERF019 plants to tolerate water-deficit stress was therefore examined by exposing 21-day-old ERF019 and Col-0 plants to dehydration. Plants exposed to water-deficit stress for 12 days (Fig. 4A) were used for Fv/Fm measurements to determine photosynthetic activity. ERF019 lines showed significantly higher photosynthetic activity when comparison with Col-0 plants (Fig. 4B). At 17 days of dehydration, damage became evident and plants were re-watered. After two days of recovery, survival percentage was scored (Fig. 4B). The percentage of plants that survived the water-deficit stress was higher in ERF019-8, ERF019-7 and ERF019-6 lines at 100%, 90% and 80%, respectively, when compared with Col-0 plants of which 23% survived. There was no difference in survival percentage between Col-0 and ERF019-4 (P = 0.894).

Based on the above results, stomata from leaves of ERF019 and Col-0 were analyzed under optimal growing conditions. Col-0 plant stomata were significantly more open than stomata of ERF019 lines (Fig. 4C). The average stomatal aperture ratio (width/length) in ERF019 lines ranged from 0.09 to 0.11, while the mean stomatal aperture in Col-0 was around 0.23. The density of guard cells, counted per unit area, was not different between ERF019 lines and Col-0 plants (data not shown).

Cuticular and cell wall permeability may contribute to enhanced water-deficit stress tolerance. We therefore assayed chlorophyll leaching in ERF019 lines. This technique is frequently used to examine cuticle/cell wall permeability alteration in leaves (Chen *et al.*, 2003). Compared with Col-0 plants, chlorophyll was extracted more slowly from all ERF019 plants lines, with the exception of the ERF019-4 line (Fig. 4D).

Comparative proteomic analysis of Col-0 and ERF019-7 plant leaves under optimal and water-deficit conditions

Arabidopsis plants were subjected to a controlled water-deficit treatment that consisted of withholding water from 21-day-old plants by maintaining the soil humidity at a target level corresponding to a moderate water deficit for 15 days. To confirm the efficacy of the water-deficit stress treatment, analyses of pigment content, proline levels, and SOD activity were carried out (see Supplementary Fig. S6).

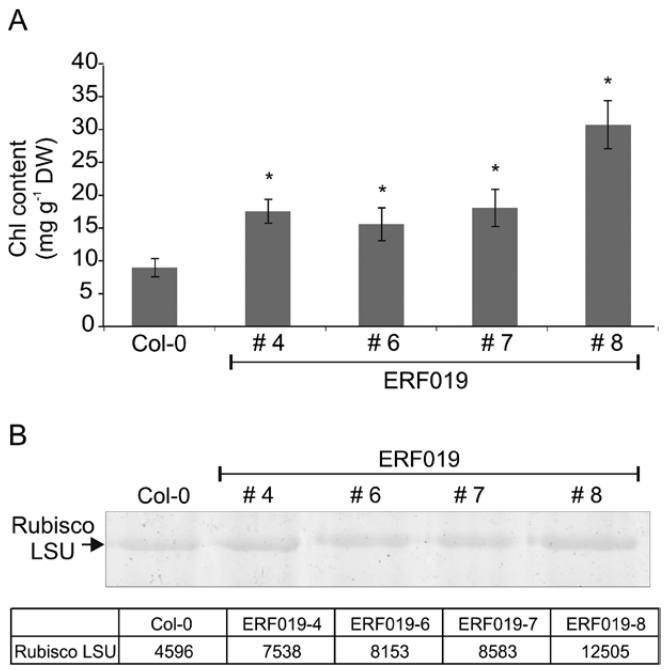

	Col-0	ERF019-4	ERF019-6	ERF019-7	ERF019-8
Rubisco LSU	4596	7538	8153	8583	12505

Fig. 3. Dark-induced leaf senescence of plants of Col-0 and ERF019 lines. Twenty-one-day-old plants of Col-0 and ERF019 kept in darkness for 3 to 4 days were used. (A) Chlorophyll content values are given as mg of total chlorophyll per 1 g of leaf DW. The error bars indicate the sample SE (n=4). The asterisks over the error bars indicate a significant difference between plants of ERF019 lines and Col-0 (P<0.005). (B) Rubisco LSU content among the different samples by Coomassie blue-stained SDS-PAGE. Each line contains protein extracts corresponding to 0.4 mg DW from plants of Col-0 and ERF019-4, -6, -7 and -8 lines subjected to dark-induced senescence. The table below shows Rubisco LSU relative abundance quantified by digitalization normalized to mg of DW and expressed as a ratio of arbitrary units for pixel intensities. (This figure is available in colour at *JXB* online.)

Higher chlorophyll content was detected in the ERF019-7 line relative to Col-0 in both control and water-deficit stress conditions, but no changes were observed between treatments in all lines (Supplementary Fig. S6A). Proline levels were similar in Col-0 and ERF019-7 under control conditions. When these plants were subjected to water stress, proline levels increased almost three-fold in Col-0 but no significant change was observed in the ERF019-7 line (Supplementary Fig. S6B). Comparing the four samples, no differences in SOD activity levels were detected (Supplementary Fig. S6C).

Plants of Col-0 and ERF019-7 that were subjected to this controlled water-deficit stress treatment and grown under optimal conditions were used to perform bottom-up proteomics. We decided to use ERF019-7 in preference to the other transgenic lines as this line showed an intermediate phenotype that is consistent with the level of *AtERF019* overexpression. The total number of proteins identified from these samples was 998 (see Supplementary Table S2). Proteomic data sets were also interpreted using the MapMan bin system for functional classification (Thimm *et al.*, 2004). We were able to functionally categorize all of the proteins identified (see Supplementary Fig. S7). The functional category with the second highest number of proteins was the stress and redox homeostasis (Supplementary Fig. S7).

Comparison analyses were performed between the proteomes of Col-0 and ERF019-7 in both control and water-deficit stress conditions and presented using a four-way Venn diagram that shows all of the 15 possible overlaps between datasets (Fig. 5A). Proteins that are unique to each sample are also listed (Fig. 5B). Eleven proteins were detected solely in the ERF019-7 control sample and four only in the water-deficit stress samples of ERF019-7. Among them were stress-related proteins such as chloroplastic betaine aldehyde dehydrogenase 1 (ALDH, Q9S795), reticulon-like protein B2 (RTNLB2, Q9SUT9); BCAT3 (Q9M401), the zin finger transcription factor OXS2 (P93755), and nudix hydrolase 2 (AtNUDX2, Q94B74). Additionally, several genes encoding proteins present only in ERF019-7 control or water-deficit stress samples and not in Col-0, were found to be targets of AtERF019, as revealed by a global survey of the Arabidopsis genome using the publicly available database (http://neomorph.salk.edu/PlantCistromeDB) (O´Malley *et al.*, 2016). The predicted targets include genes encoding OXS2 (*At2g41900*), MTHFR2 (*At2g44160*), KORRIGAN (*At5g49720*), CalS12 (*At4g03550*), and AtBGAL10 (*At5g63810*) (see Supplementary Table S3). Genes of the AP2/ERF family were also detected as predicted targets of AtERF019, including *ERF3* (*At1g50640*), *ERF6* (*At4g17490*), *ERF8* (*At1g53170*) and *ERF11* (*At1g28370*).

To gather more information about the role of these proteins in water-deficit stress, T-DNA insertion mutants for *BCAT3* and *RTNLB2* genes were obtained from the Arabidopsis Biological Resource Center and genotyped to obtain homozygous lines. Plants of Col-0, *bcat3*, and *rtnlb2* mutants were subjected to controlled water-deficit stress treatment (see Supplementary Fig. S8). During this treatment, plants did not die but growth and seed yield were affected. At the end of the life cycle, *bcat3* plants yielded significantly fewer seeds than Col-0 and *rtnlb2* (Supplementary Fig. S8). The difference in seed yield in the wild type and T-DNA insertion lines grown under non-stressful conditions was not statistically significant (data not shown).

Discussion

Previous data showed the rapid accumulation of *AtERF019* transcripts after methyl viologen treatment of Arabidopsis leaves, which disappeared 24 h after treatment (Scarpeci *et al.*, 2008). This could be explained by the fact that *AtERF019* is an intronless gene, which could generate less stable mRNA transcripts (Narsai *et al.*, 2007). These data suggested that *AtERF019* gene expression is not only regulated by oxidative stress at the transcriptional level but that mRNA stability might also be affected under this condition. Here, overexpression of *AtERF019* in Arabidopsis ERF019 lines led to an enhancement of water stress tolerance and a delay in flowering time and senescence. On the other hand, the size of ERF019 plant lines was inversely correlated with the level of *AtERF019* overexpression (Fig. 1A-C). Overexpression of the *AtERF019* gene may cause an inhibition in cell expansion that could be lethal depending on the level of expression.

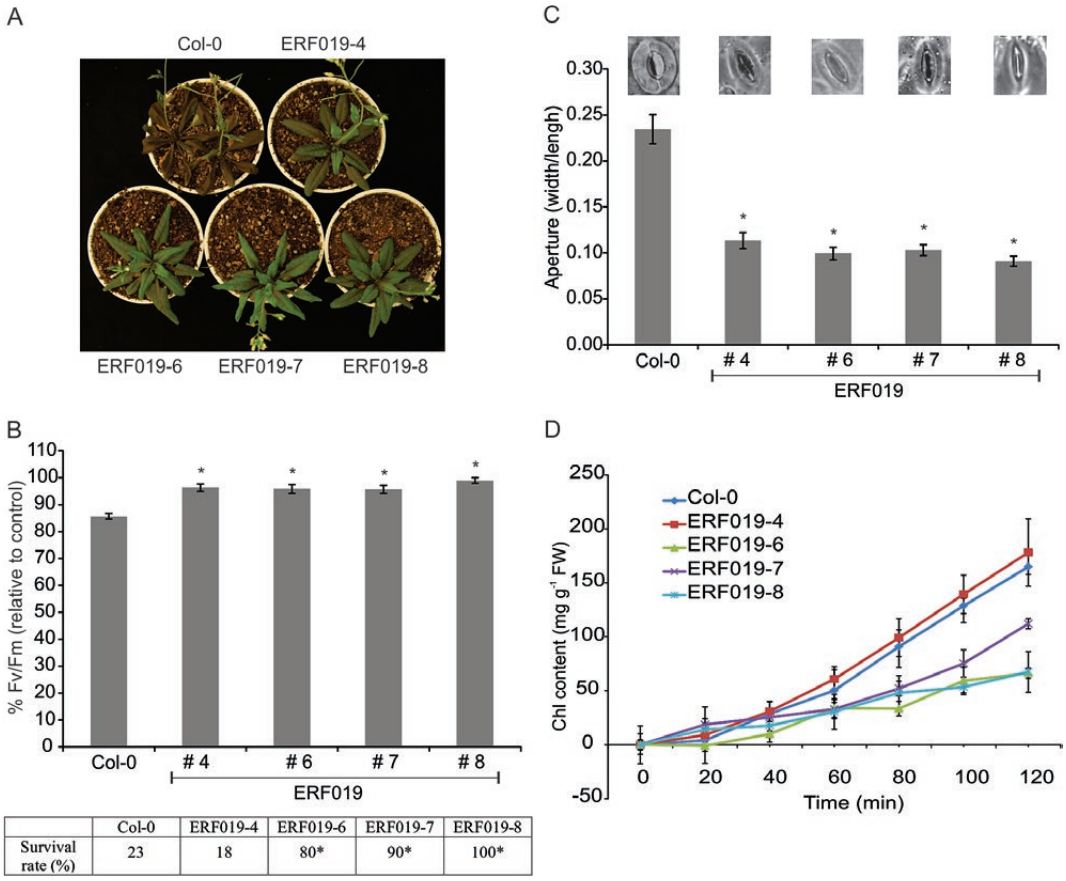

	Col-0	ERF019-4	ERF019-6	ERF019-7	ERF019-8
Survival rate (%)	23	18	80*	90*	100*

Fig. 4. Water-deficit stress tolerance of ERF019 lines. Col-0 and transgenic plants were grown in soil under optimal conditions. When the plants were 21 days old, water was withheld from plants. (A) Representative photographs of plants exposed to water-deficit stress for 12 days and used for Fv/Fm measurements. (B) Chlorophyll fluorescence was measured in the sixth and the eighth detached leaf of 21-day-old Arabidopsis plants exposed for 12 days to water-deficit stress, and Fv/Fm was calculated. The error bars indicate the sample SE (n=4). The asterisks over the error bars indicate a significant difference between ERF019 lines and Col-0 plants (P<0.001). Plants of ERF019 and Col-0 subjected to water-deficit stress were watered again after 17 days. Survival rate was calculated two days later using ten plants per genotype and the experiment was performed three times. The asterisks indicate a significant difference between ERF019 lines and Col-0 plants (P< 0.01). (C) Stomatal aperture was determined from images of silicone rubber imprints of the abaxial surfaces of the third and fourth leaf from 21-day-old ERF019 and Col-0 plants grown under optimal conditions. Inset: an imprint of representative stomata of Col-0 plants and ERF019 lines (each photo represents a width of 15 µm). The error bars indicate the sample SE (n= 40–60). The asterisks over the error bars indicate a significant difference between ERF019 lines and Col-0 plants (P<0.001). (D) Chlorophyll leaching assays were carried out using 4-week old Col-0 and ERF019 plants immersed in 80% ethanol for different time intervals. The results are derived from three independent experiments and depicted with SEM for each time point.

This could also explain the pronounced dwarf phenotype in certain ERF019 lines. The dwarf phenotype was previously observed in transgenic Arabidopsis plants overexpressing *ERF6* and was suppressed by overexpression of the *ERF11* repressor (Dubois *et al.*, 2015). Other mutants showed this characteristic plant stress-related phenotype (Chaves *et al.*, 2002). Plants overexpressing *CBF1-3* genes in Arabidopsis not only resulted in growth retardation and dwarfism but also in frost tolerance (Liu *et al.*, 1998; Gilmour *et al.*, 2004).

Adult ERF019 lines showed leaf curling and smaller rosette size, with increased leaf number, compared with Col-0 plants (Supplementary Fig. S1). Similar results were reported for the accession C24 (Bechtold *et al.*, 2010), suggesting that plants reduce water loss by altering vegetative growth. Furthermore, ERF019 lines presented abnormalities in cotyledons venation patterning and a more acute silique angle than those of Col-0 plants (Supplementary Fig. S2). Defects in leaf size and shape are often a consequence of disruption of the vascular pattern (Dengler and Kang, 2001). These data showed that constitutive expression of *AtERF019* caused several pleiotropic effects on plant growth and development, which might be related to alterations in auxin signaling. In fact, changes in cotyledon venation pattern and angle of silique formation were previously reported in the auxin-resistant mutant *axr6* (Hobbie *et al.*, 2000). Recently, several reports have indicated a role for auxin in senescence regulation, although their precise mode of action remains vaguely defined at present (Mueller-Roeber and Balazadeh, 2014).

Plants of 63-day-old ERF019 lines retained a higher level of chlorophyll in comparison to Col-0 (Fig. 2A and 2B) indicating that *AtERF019* overexpression elicited a delay in natural leaf senescence (Supplementary Fig. S1B). Overexpression of *AtERF019* delayed flowering and extended plant longevity for 2 weeks. The results shown in Figure 2A might therefore have been the consequence of both late flowering and a delay in the onset of leaf senescence. Furthermore, the extended

A

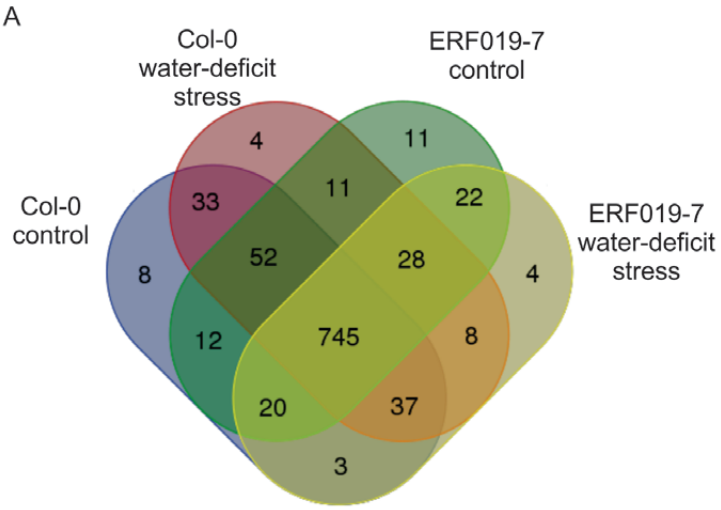

B

Elements only in Col-0 control	Elements only in Col-0 water-deficit stress	Elements only in ERF019-7 control	Elements only in ERF019-7 water-deficit stress
Q9SVC2, Syntaxin-122	Q04980, Low-temperature-induced 65 kDa protein	Q9SZN1, V-type proton ATPase subunit B2	Q8VY88, Protein LHCP translocation defect
Q9T0K7, 3-hydroxyisobutyryl-CoA hydrolase-like protein 3, mitochondrial	Q42599, NADH dehydrogenase [ubiquinone] iron-sulfur protein 8-A mitochondrial	Q8H118, Probable methyltransferase PMT1	Q94B74, Nudix hydrolase 2
P56795, 50S ribosomal protein L22, chloroplastic	Q9S7Z3, Glutathione gamma-glutamylcysteinyltransferase 1	Q9S795, Betaine aldehyde dehydrogenase 1, chloroplastic	O23365, Cytochrome P450 97B3, chloroplastic
Q9M8S8, Inositol-phosphate phosphatase	P49077, Aspartate carbamoyltransferase, chloroplastic	Q9CAF5, ABC transporter I family member 6, chloroplastic	Q9LXZ5, Alpha-soluble NSF attachment protein 1
Q9FZ48, Ubiquitin-conjugating enzyme E2 36		Q9SUT9, Reticulon-like protein B2	
Q39241, Thioredoxin H5		P0CZ23, Acyl-coenzyme A oxidase 3, peroxisomal	
Q9LQU2, Protein Plant cadmium resistance 1		Q9M401, Branched-chain-amino-acid aminotransferase 3	
Q08298, Dehydration-responsive protein RD22		P93755, Zinc finger CCCH domain-containing protein 30	
		Q9SZD4, 26S proteasome regulatory subunit 4 homolog A	
		Q9XF11, UPF0496 protein	
		Q43387, Peroxidase 71	

Fig. 5. Comparative analysis of the leaf proteomes of Col-0 and ERF019-7 plants under control and water-deficit stress conditions. (A) Four-way Venn diagram showing the relationship between proteins identified by the bottom-up assay in the following samples: Col-0 control, Col-0 water-deficit stress, ERF019-7 control and ERF019-7 water-deficit stress. (B) List of unique proteins in each group. (This figure is available in colour at *JXB* online.)

delay in senescence observed in ERF019-6, -7 and -8 plants, coincided with several biochemical parameters assayed such as protein degradation, Rubisco LSU and GS1 and GS2 content (Fig. 2C-E). Masclaux *et al.* (2000) showed that in senescing tobacco a decrease in GS2 contrasted with a simultaneous increase of GS1. In addition, transcriptomic analyses have revealed the existence of crosstalk between stress responses and leaf senescence (Lim and Ng, 2007). Furthermore, Arabidopsis mutants such as *ore1*, *ore3,* and *ore9*, which exhibit a delayed senescence and prolonged lifespan, were found to be more tolerant to oxidative stresses (Woo *et al.*, 2004). Young seedlings, 10–15 days old, of both Col-0 and ERF019 showed a similar behavior when subjected to drought or dark-induced senescence treatments (data not shown, Supplementary Fig. S4). Thus, it may be possible that AtERF019 interacts with downstream gene targets modulating stress responses coordinately with the developmental program. In fact, *ERF11* together with *ERF8* were found to be direct targets of AtERF019 and both partially rescued the dwarf phenotype of a gibberellin impaired mutant (Zhou *et al.*, 2016).

Plant tolerance responses to water-deficit conditions are exerted via several distinct mechanisms, such as stomatal regulation of transpiration, and cuticle and cell wall permeability (Kosma *et al.*, 2009; Sirichandra *et al.*, 2009). Stomata play a significant role in plant adaptation to water-deficit stress since a restriction in their aperture avoids water loss. ERF019 plants had lower cuticle and cell wall permeability

and a smaller stomatal aperture, two characteristics associated with water-deficit stress tolerance responses. The fact that ERF019 lines have smaller stomata aperture under optimal growth conditions would restrict carbon dioxide intake and consequently less carbon dioxide would be fixed in the cell. For this reason the amount of biomass would be lower, leading to smaller plants. Considering that ERF019 lines have smaller stomatal apertures and a less permeable cuticle and cell wall (Fig. 4C and 4D), the transpiration rate would be lower, resulting in plants with higher tolerance to water stress than Col-0 plants.

Subtle changes rather than massive reprogramming of transcription networks is thought to occur in Arabidopsis plants subjected to water-deficit stress (Hummel *et al.*, 2010). We therefore conducted a proteomic study to gain a deeper understanding of the water-deficit stress tolerance mechanisms displayed by ERF019 plants subjected to a progressive soil water deficit. The proline content significantly increased in Col-0 water-deficit stress samples (Supplementary Fig. S6B) as expected (Hummel *et al.*, 2010), validating the water-deficit treatment performed. Using this approach, BCAT3 was one of the eleven proteins detected only in the ERF019-7 control sample. BCAT3 is localized to plastids and is involved in both branch-chain amino acid (BCAA) and glucosinolate synthesis (Diebold *et al.*, 2002; Knill *et al.*, 2008). BCAT functions in the last step of the biosynthesis of BCAAs. In Arabidopsis, the *BCAT2* gene was induced in response to dehydration stress and this fact positively correlated with the accumulation of BCAAs (Urano *et al.*, 2009). Nevertheless, the role of BCAAs in water-deficit stress tolerance is still unknown. Previous studies indicate that water-deficit stress alters the glucosinolate composition of plants and that the addition of exogenous glucosinolate hydrolysis products alleviates the adverse effects of this stress. However, the physiological role of these metabolites in response to this particular abiotic stress is still unclear (Martinez-Ballesta *et al.*, 2013). Since the *bcat3* T-DNA insertion line was more sensitive to water-deficit stress than Col-0 plants (Supplementary Fig. S8) and considering that BCAT3 protein accumulated at higher levels under control conditions in ERF019 plants compared to Col-0 plants, it could be argued that glucosinolates and BCAAs contributed to the higher tolerance to water-deficit stress shown by the *AtERF019* overexpressing plants.

The zinc finger transcription factor OXS2 was another protein present in ERF019-7 plants but not in Col-0 plants under control growth conditions. The gene encoding OXS2 is predicted to be a direct target of AtERF019 (Supplementary Table S3). OXS2 has been found to have multiple roles, such as the maintenance of vegetative growth, the activation of stress tolerance, and the control of stress-induced reproduction. Blanvillain *et al.* (2011) reported that the cytoplasmic form of OXS2 could be involved in floral repression by an unknown mechanism, and that it is translocated to the nucleus upon stress activation. In line with this model, the presence of OXS2 in the ERF019-7 plant could extend vegetative growth by suppressing floral transition (see Supplementary Fig. S9) and by activating stress tolerance through the modified expression of genes associated with this response.

Arabidopsis plants do not accumulate glycine betaine in response to osmotic stress, even though their genome contains two genes, *ALDH10A8* and *ALDH10A9*, which code for ALDH (Missihoun *et al.*, 2011). ALDH10A8 was one of the proteins detected exclusively in the ERF019-7 control sample. Previous studies showed that the inactivation of *ALDH10A8* rendered Arabidopsis plants more sensitive to drought and excess salt, possibly due to increased intracellular levels of toxic aminoaldehydes in the knock-out mutant (Missihoun *et al.*, 2011). The authors hypothesized that ALDH10A8 may serve as a detoxification enzyme controlling aminoaldehyde levels, and that this function could ameliorate the effects of drought stress in ERF019 lines.

The AtNUD2X2 protein was only present in ERF019-7 plants subjected to water-deficit stress. Ogawa *et al.* (2009) showed that the expression of *AtNUDX2* was similarly induced by treatment with methyl viologen, drought and salinity conditions. Furthermore, overexpression of *AtNUDX2*, encoding an ADP-ribose pyrophosphatase, enhances Arabidopsis plant tolerance to oxidative stress. This is due to the maintenance of NAD^+ and ATP levels by nucleotide recycling from free ADP-ribose molecules under stress conditions (Ogawa *et al.*, 2009). For this reason, AtNUD2X2 could be in part responsible for the higher tolerance of ERF019 lines to water-deficit stress.

Four proteins related to cell wall synthesis and metabolism - MTHFR2, CalS12, KORRIGAN, and AtBGAL10 - were notably also found to accumulate in ERF019-7 plant samples but not in Col-0 (Supplementary Table S2). Interestingly, the genes encoding these proteins were also found to be direct targets of AtERF019 in the Plant Cistrome database (O´Malley *et al.*, 2016; Supplementary Table S3). Firstly, MTHFR2 is involved in lignin accumulation (Tang *et al.*, 2014), a response believed to prevent cell wall damage when plants are exposed to water-deficit stress (Lee *et al.*, 2007). Secondly, CalS12 is associated with callose deposition (Flors *et al.*, 2005), which has been associated with drought protection by increasing the water holding capacity of plants (Ahmed *et al.*, 2015). KORRIGAN has been shown to play a significant role in cellulose biosynthesis (Maloney and Mansfield, 2010), though its function in drought stress remains unclear. Finally, AtBGAL10 is an enzyme responsible for most of the β-Galactosidase activity against xyloglucan in Arabidopsis and may therefore be implicated in the modification of xyloglucan structure via the hydrolysis of the abundant β-Galactose units that comprise the xyloglucan side chains (Sampedro *et al.*, 2012). Even though little is known about changes in the cell wall itself, it is evident that these modifications may be important during the adaption of plant cells to water-deficit stress.

Overall, in light of the present findings, it is suggested that upon exposure to water-deficit stress, plants increase drought tolerance by inducing *AtERF019* to strengthen their chances of reproductive success. This tolerance can be explained at the physiological level as ERF019 plants have smaller stomatal apertures and a less permeable cuticle and cell wall than Col-0 plants, resulting in a lower transpiration rate. At the molecular level, the enhanced performance of ERF019 plants under

water-deficit stress could be explained by the higher amount of proteins involved in stress tolerance, such as BCAT3 and OXS2, and by cell wall metabolism (Supplementary Fig. S9). Finally, the finding that overexpression of *AtERF019* gives rise to drought tolerance and delayed leaf senescence supports the 'stress resistance' theory of aging in plants (Sharabi-Schwager *et al.*, 2010). This theory states that an enhanced resistance to internal or external stress also prolongs lifespan and longevity, supporting the possibility of crosstalk between the signaling pathways that regulate stress tolerance and senescence processes.

Supplementary data

Supplementary data are available at *JXB* online

Fig. S1. Transgenic plants constitutively overexpressing *AtERF019*.

Fig. S2. Characterization of the vascular pattern and angle formed between the silique and the inflorescence stem of ERF019 lines.

Fig. S3. Analysis of leaf pigment levels of Col-0 plants and ERF019 lines grown under optimal conditions.

Fig. S4. Chlorophyll content of Col-0 plants and ERF019 lines after dark-induced senescence.

Fig. S5. Heat map changes in the steady state level of *AtERF019* transcripts in response to different stress sources and treatments.

Fig. S6. Chlorophyll, proline, and SOD content of Col-0 and ERF019-7 plants under control or water-deficit stress conditions.

Fig. S7. Functional categories for leaf proteins from Col-0 and ERF019-7 plants detected by nanoLC-Orbitrap tandem mass spectrometry.

Fig. S8. Seed production after water-deficit treatment.

Fig. S9. Proposed model for the function of AtERF019 in water-deficit stress.

Table S1. List of primers used in this study.

Table S2. List of proteins identified using Scaffold software.

Table S3. Predicted target genes of AtERF019.

Acknowledgments

This work was supported by ANPCyT and CONICET from Argentina. TES was supported by a short-term Fulbright-CONICET fellowship. We thank Prof. Dr. Bernd Mueller-Roeber for his collaboration in producing transgenic ERF019 lines and Dr. Neil Kelleher and all the members of his group from Northwestern Proteomics (Northwestern University, USA) for technical advice on bottom-up proteomics.

References

Abogadallah GM, Nada RM, Malinowski R, Quick P. 2011. Overexpression of HARDY, an AP2/ERF gene from Arabidopsis, improves drought and salt tolerance by reducing transpiration and sodium uptake in transgenic Trifolium alexandrinum L. Planta **233,** 1265–1276.

Ahmed IM, Nadira UA, Bibi N, Cao F, He X, Zhang G, Wu F. 2015. Secondary metabolism and antioxidants are involved in the tolerance to drought and salinity, separately and combined, in Tibetan wild barley. Environmental and Experimental Botany **111,** 1–12.

Amalraj A, Luang S, Kumar MY, *et al.* 2016. Change of function of the wheat stress-responsive transcriptional repressor TaRAP2.1L by repressor motif modification. Plant Biotechnology Journal **14,** 820–832.

Baker NR, Rosenqvist E. 2004. Applications of chlorophyll fluorescence can improve crop production strategies: an examination of future possibilities. Journal of Experimental Botany **55,** 1607–1621.

Bates LS, Waldran RP, Teare ID. 1973. Rapid determination of free proline in water stress studies. Plant and Soil **39,** 205–208.

Beauchamp C, Fridovich I. 1971. Superoxide dismutase: improved assays and an assay applicable to acrylamide gels. Analytical Biochemistry **44,** 276–287.

Bechtold U, Lawson T, Mejia-Carranza J, Meyer RC, Brown IR, Altmann T, Ton J, Mullineaux PM. 2010. Constitutive salicylic acid defences do not compromise seed yield, drought tolerance and water productivity in the Arabidopsis accession C24. Plant, Cell & Environment **33,** 1959–1973.

Blanvillain R, Wei S, Wei P, Kim JH, Ow DW. 2011. Stress tolerance to stress escape in plants: role of the OXS2 zinc-finger transcription factor family. The EMBO journal **30,** 3812–3822.

Boyer JS, Bowen BL. 1970. Inhibition of oxygen evolution in chloroplasts isolated from leaves with low water potentials. Plant Physiology **45,** 612–615.

Boyer JS. 1982. Plant productivity and environment. Science **218,** 443–448.

Buchanan-Wollaston V, Earl S, Harrison E, Mathas E, Navabpour S, Page T, Pink D. 2003. The molecular analysis of leaf senescence–a genomics approach. Plant Biotechnology Journal **1,** 3–22.

Buchanan-Wollaston V, Page T, Harrison E, *et al.* 2005. Comparative transcriptome analysis reveals significant differences in gene expression and signalling pathways between developmental and dark/starvation-induced senescence in Arabidopsis. The Plant Journal **42,** 567–585.

Bumpus SB, Evans BS, Thomas PM, Ntai I, Kelleher NL. 2009. A proteomics approach to discovering natural products and their biosynthetic pathways. Nature Biotechnology **27,** 951–956.

Cao PB, Azar S, SanClemente H, Mounet F, Dunand C, Marque G, Marque C, Teulières C. 2015. Genome-wide analysis of the AP2/ERF family in Eucalyptus grandis: an intriguing over-representation of stress-responsive DREB1/CBF genes. PLoS ONE **10,** e0121041.

Chaves MM, Pereira JS, Maroco J, Rodrigues ML, Ricardo CP, Osório ML, Carvalho I, Faria T, Pinheiro C. 2002. How plants cope with water stress in the field. Photosynthesis and growth. Annals of Botany **89 Spec No,** 907–916.

Chen X, Goodwin SM, Boroff VL, Liu X, Jenks MA. 2003. Cloning and characterization of the WAX2 gene of Arabidopsis involved in cuticle membrane and wax production. The Plant Cell **15,** 1170–1185.

Claeys H, Inzé D. 2013. The agony of choice: how plants balance growth and survival under water-limiting conditions. Plant Physiology **162,** 1768–1779.

Clough SJ, Bent AF. 1998. Floral dip: a simplified method for Agrobacterium-mediated transformation of *Arabidopsis thaliana*. The Plant Journal **16,** 735–743.

Dangl JL, Dietrich RA, Thomas H. 2000. Senescence and programmed cell death. B Buchanan, W Gruissem, R Jones, eds, Biochemistry and Molecular Biology of Plants. Rockville, MD: American Society of Plant Physiologists Press, 1044–1100.

Dengler N, Kang J. 2001. Vascular patterning and leaf shape. Current opinion in plant biology **4,** 50–56.

Diebold R, Schuster J, Däschner K, Binder S. 2002. The branched-chain amino acid transaminase gene family in Arabidopsis encodes plastid and mitochondrial proteins. Plant Physiology **129,** 540–550.

Dong CJ, Liu JY. 2010. The Arabidopsis EAR-motif-containing protein RAP2.1 functions as an active transcriptional repressor to keep stress responses under tight control. BMC Plant Biology **10,** 47.

Dubois M, Van den Broeck L, Claeys H, Van Vlierberghe K, Matsui M, Inzé D. 2015. The ETHYLENE RESPONSE FACTORs ERF6 and ERF11 antagonistically regulate mannitol-induced growth inhibition in Arabidopsis. Plant Physiology **169,** 166–179.

Flors V, Ton J, Jakab G, Mauch-Mani B. 2005. Abscisic acid and callose: team players in defence against pathogens? Journal of Phytopathology **153,** 377–383.

Fujimoto SY, Ohta M, Usui A, Shinshi H, Ohme-Takagi M. 2000. Arabidopsis ethylene-responsive element binding factors act as transcriptional activators or repressors of GCC box-mediated gene expression. The Plant Cell **12,** 393–404.

Gilmour SJ, Fowler SG, Thomashow MF. 2004. Arabidopsis transcriptional activators CBF1, CBF2, and CBF3 have matching functional activities. Plant Molecular Biology **54,** 767–781.

Gupta AS, Webb RP, Holaday AS, Allen RD. 1993. Overexpression of superoxide dismutase protects plants from oxidative stress (Induction of ascorbate peroxidase in superoxide dismutase-overexpressing plants). Plant Physiology **103,** 1067–1073.

Hobbie L, McGovern M, Hurwitz LR, Pierro A, Liu NY, Bandyopadhyay A, Estelle M. 2000. The *axr6* mutants of Arabidopsis thaliana define a gene involved in auxin response and early development. Development **127,** 23–32.

Hummel I, Pantin F, Sulpice R, *et al*. 2010. Arabidopsis plants acclimate to water deficit at low cost through changes of carbon usage: an integrated perspective using growth, metabolite, enzyme, and gene expression analysis. Plant Physiology **154,** 357–372.

Inzé A, Vanderauwera S, Hoeberichts FA, Vandorpe M, Van Gaever T, Van Breusegem F. 2012. A subcellular localization compendium of hydrogen peroxide-induced proteins. Plant, cell & environment **35,** 308–320.

Keller A, Nesvizhskii AI, Kolker E, Aebersold R. 2002. Empirical statistical model to estimate the accuracy of peptide identifications made by MS/MS and database search. Analytical Chemistry **74,** 5383–5392.

Knill T, Schuster J, Reichelt M, Gershenzon J, Binder S. 2008. Arabidopsis branched-chain aminotransferase 3 functions in both amino acid and glucosinolate biosynthesis. Plant Physiology **146,** 1028–1039.

Kosma DK, Bourdenx B, Bernard A, Parsons EP, Lü S, Joubès J, Jenks MA. 2009. The impact of water deficiency on leaf cuticle lipids of Arabidopsis. Plant Physiology **151,** 1918–1929.

Lee BR, Kim KY, Jung WJ, Avice JC, Ourry A, Kim TH. 2007. Peroxidases and lignification in relation to the intensity of water-deficit stress in white clover (*Trifolium repens* L.). Journal of experimental botany **58,** 1271–1279.

Lers A. 2007. Environmental regulation of leaf senescence. In: Annual Plant Reviews. Senescence Processes in Plants, Blackwell Publishing Ltd **26,** 108–144.

Li Z, Zhang L, Yu Y, Quan R, Zhang Z, Zhang H, Huang R. 2011. The ethylene response factor AtERF11 that is transcriptionally modulated by the bZIP transcription factor HY5 is a crucial repressor for ethylene biosynthesis in Arabidopsis. The Plant Journal **68,** 88–99.

Licausi F, Ohme-Takagi M, Perata P. 2013. APETALA2/Ethylene Responsive Factor (AP2/ERF) transcription factors: mediators of stress responses and developmental programs. The New phytologist **199,** 639–649.

Lichtenthaler HK, Buschmann C, Rinderle U, Schmuck G. 1986. Application of chlorophyll fluorescence in ecophysiology. Radiation and Environmental Biophysics **25,** 297–308.

Lim CA, Ng HH. 2007. Application of advanced technologies in ageing research. Mechanisms of ageing and development **128,** 149–160.

Liu Q, Kasuga M, Sakuma Y, Abe H, Miura S, Yamaguchi-Shinozaki K, Shinozaki K. 1998. Two transcription factors, DREB1 and DREB2, with an EREBP/AP2 DNA binding domain separate two cellular signal transduction pathways in drought- and low-temperature-responsive gene expression, respectively, in Arabidopsis. The Plant Cell **10,** 1391–1406.

Maloney VJ, Mansfield SD. 2010. Characterization and varied expression of a membrane-bound endo-beta-1,4-glucanase in hybrid poplar. Plant Biotechnology Journal **8,** 294–307.

Masclaux C, Valadier MH, Brugière N, Morot-Gaudry JF, Hirel B. 2000. Characterization of the sink/source transition in tobacco (*Nicotiana tabacum* L.) shoots in relation to nitrogen management and leaf senescence. Planta **211,** 510–518.

Missihoun TD, Schmitz J, Klug R, Kirch HH, Bartels D. 2011. Betaine aldehyde dehydrogenase genes from Arabidopsis with different sub-cellular localization affect stress responses. Planta **233,** 369–382.

Mizoi J, Shinozaki K, Yamaguchi-Shinozaki K. 2012. AP2/ERF family transcription factors in plant abiotic stress responses. Biochimica et Biophysica Acta **1819,** 86–96.

Mueller-Roeber B, Balazadeh S. 2014. Auxin and its role in plant senescence. Journal of Plant Growth Regulation **33,** 21–33.

Munné-Bosch S, Alegre L. 2004. Die and let live: leaf senescence contributes to plant survival under drought stress. Functional Plant Biology **31,** 203–216.

Nakano T, Suzuki K, Fujimura T, Shinshi H. 2006. Genome-wide analysis of the ERF gene family in Arabidopsis and rice. Plant Physiology **140,** 411–432.

Narsai R, Howell KA, Millar AH, O'Toole N, Small I, Whelan J. 2007. Genome-wide analysis of mRNA decay rates and their determinants in Arabidopsis thaliana. The Plant Cell **19,** 3418–3436.

Nesvizhskii AI, Keller A, Kolker E, Aebersold R. 2003. A statistical model for identifying proteins by tandem mass spectrometry. Analytical Chemistry **75,** 4646–4658.

Ogawa T, Ishikawa K, Harada K, Fukusaki E, Yoshimura K, Shigeoka S. 2009. Overexpression of an ADP-ribose pyrophosphatase, AtNUDX2, confers enhanced tolerance to oxidative stress in Arabidopsis plants. The Plant Journal **57,** 289–301.

Ohta M, Matsui K, Hiratsu K, Shinshi H, Ohme-Takagi M. 2001. Repression domains of class II ERF transcriptional repressors share an essential motif for active repression. The Plant Cell **13,** 1959–1968.

O'Malley RC, Huang SS, Song L, Lewsey MG, Bartlett A, Nery JR, Galli M, Gallavotti A, Ecker JR. 2016. Cistrome and epicistrome features shape the regulatory DNA landscape. Cell **165,** 1280–1292.

Osakabe Y, Osakabe K, Shinozaki K, Tran LS. 2014. Response of plants to water stress. Frontiers in Plant Science **5,** 86.

Park JM, Park CJ, Lee SB, Ham BK, Shin R, Paek KH. 2001. Overexpression of the tobacco Tsi1 gene encoding an EREBP/AP2-type transcription factor enhances resistance against pathogen attack and osmotic stress in tobacco. The Plant Cell **13,** 1035–1046.

Rivero RM, Kojima M, Gepstein A, Sakakibara H, Mittler R, Gepstein S, Blumwald E. 2007. Delayed leaf senescence induces extreme drought tolerance in a flowering plant. Proceedings of the National Academy of Sciences of the United States of America **104,** 19631–19636.

Sakuma Y, Liu Q, Dubouzet JG, Abe H, Shinozaki K, Yamaguchi-Shinozaki K. 2002. DNA-binding specificity of the ERF/AP2 domain of Arabidopsis DREBs, transcription factors involved in dehydration- and cold-inducible gene expression. Biochemical and biophysical research communications **290,** 998–1009.

Sampedro J, Gianzo C, Iglesias N, Guitián E, Revilla G, Zarra I. 2012. AtBGAL10 is the main xyloglucan β-galactosidase in Arabidopsis, and its absence results in unusual xyloglucan subunits and growth defects. Plant Physiology **158,** 1146–1157.

Scarpeci TE, Marro ML, Bortolotti S, Boggio SB, Valle EM. 2007. Plant nutritional status modulates glutamine synthetase levels in ripe tomatoes (*Solanum lycopersicum* cv. Micro-Tom). Journal of Plant Physiology **164,** 137–145.

Scarpeci TE, Zanor MI, Carrillo N, Mueller-Roeber B, Valle EM. 2008. Generation of superoxide anion in chloroplasts of *Arabidopsis thaliana* during active photosynthesis: a focus on rapidly induced genes. Plant Molecular Biology **66,** 361–378.

Scarpeci TE, Zanor MI, Mueller-Roeber B, Valle EM. 2013. Overexpression of AtWRKY30 enhances abiotic stress tolerance during early growth stages in Arabidopsis thaliana. Plant Molecular Biology **83,** 265–277.

Sedmak JJ, Grossberg SE. 1977. A rapid, sensitive, and versatile assay for protein using Coomassie brilliant blue G250. Analytical biochemistry **79,** 544–552.

Semiarti E, Ueno Y, Tsukaya H, Iwakawa H, Machida C, Machida Y. 2001. The ASYMMETRIC LEAVES2 gene of Arabidopsis thaliana regulates formation of a symmetric lamina, establishment of venation and repression of meristem-related homeobox genes in leaves. Development **128,** 1771–1783.

Sharabi-Schwager M, Lers A, Samach A, Guy CL, Porat R. 2010. Overexpression of the CBF2 transcriptional activator in Arabidopsis delays leaf senescence and extends plant longevity. Journal of Experimental Botany **61,** 261–273.

Sirichandra C, Wasilewska A, Vlad F, Valon C, Leung J. 2009. The guard cell as a single-cell model towards understanding drought tolerance and abscisic acid action. Journal of Experimental Botany **60,** 1439–1463.

Skirycz A, Reichelt M, Burow M, *et al*. 2006. DOF transcription factor AtDof1.1 (OBP2) is part of a regulatory network controlling glucosinolate biosynthesis in Arabidopsis. The Plant Journal **47,** 10–24.

Sprinthall RC. 2002. *Basic statistical analysis.* Upper Saddle River, NJ: Pearson Education Group.

Tang HM, Liu S, Hill-Skinner S, Wu W, Reed D, Yeh C-T, Nettleton D, Schnable P. 2014. The maize brown midrib2 (*bm2*) gene encodes a methylenetetrahydrofolate reductase that contributes to lignin accumulation. The Plant Journal **77,** 380–392.

Tenhaken R. 2015. Cell wall remodeling under abiotic stress. Frontiers in Plant Science **5,** 771.

Thimm O, Blasing O, Gibon Y, Nagel A, Meyer S, Kruger P, Selbig J, Muller LA, Rhee SY, Stitt M. 2004. MAPMAN: a user-driven tool to display genomics data sets onto diagrams of metabolic pathways and other biological processes. The Plant Journal **37,** 914–939.

Tsutsui T, Kato W, Asada Y, *et al*. 2009. DEAR1, a transcriptional repressor of DREB protein that mediates plant defense and freezing stress responses in Arabidopsis. Journal of Plant Research **122,** 633–643.

Ulker B, Shahid Mukhtar M, Somssich IE. 2007. The WRKY70 transcription factor of Arabidopsis influences both the plant senescence and defense signaling pathways. Planta **226,** 125–137.

Urano K, Maruyama K, Ogata Y, *et al*. 2009. Characterization of the ABA-regulated global responses to dehydration in Arabidopsis by metabolomics. The Plant Journal **57,** 1065–1078.

Vanderauwera S, Suzuki N, Miller G, *et al*. 2011. Extranuclear protection of chromosomal DNA from oxidative stress. Proceedings of the National Academy of Sciences of the United States of America **108,** 1711–1716.

Wang H, Wang H, Shao H, Tang X. 2016. Recent advances in utilizing transcription factors to improve plant abiotic stress tolerance by transgenic technology. Frontiers in Plant Science **7,** 67.

Weyers JDB, Johansen LG. 1985. Accurate estimation of stomatal aperture from silicone rubber impressions. New Phytologist **101,** 109–115.

Woo HR, Kim JH, Nam HG, Lim PO. 2004. The delayed leaf senescence mutants of Arabidopsis, ore1, ore3, and ore9 are tolerant to oxidative stress. Plant & cell physiology **45,** 923–932.

Xiong L, Wang RG, Mao G, Koczan JM. 2006. Identification of drought tolerance determinants by genetic analysis of root response to drought stress and abscisic Acid. Plant Physiology **142,** 1065–1074.

Yang SD, Seo PJ, Yoon HK, Park CM. 2011. The Arabidopsis NAC transcription factor VNI2 integrates abscisic acid signals into leaf senescence via the COR/RD genes. The Plant Cell **23,** 2155–2168.

Zhou X, Zhang ZL, Park J, *et al*. 2016. The ERF11 transcription factor promotes internode elongation by activating gibberellin biosynthesis and signaling. Plant Physiology **171,** 2760–2770.

Zimmermann P, Hirsch-Hoffmann M, Hennig L, Gruissem W. 2004. GENEVESTIGATOR. Arabidopsis microarray database and analysis toolbox. Plant Physiology **136,** 2621–2632.